

Solution Chemistry of Element 106: Theoretical Predictions of Hydrolysis of Group 6 Cations Mo, W, and Sg

V. Pershina* and J. V. Kratz

Institut für Kernchemie, Universität Mainz, 55099 Mainz, Germany

Received April 6, 2000

Fully relativistic molecular density-functional calculations of the electronic structure of hydrated and hydrolyzed complexes have been performed for the group 6 elements Mo, W, and element 106, Sg. By use of the electronic density distribution data, relative values of the free energy changes and constants of hydrolysis reactions were defined. The results show hydrolysis of the cationic species with the formation of neutral molecules to decrease in the order Mo > W > Sg, which is in agreement with experiments for Mo, W, and Sg. For the further hydrolysis process with the formation of anionic species, the trend is reversed: Mo > Sg > W. A decisive energetic factor in the hydrolysis process proved to be a predominant electrostatic metal–ligand interaction.

I. Introduction

Continuous progress in the discovery of the heaviest man-made elements¹ gives impact to both the experimental and theoretical investigations of their chemical and physicochemical properties. The production of long-lived isotopes makes it now possible to investigate the chemical behavior of such heavy elements as elements 106, 107, and 108.^{2–4} Two of these types experiments are known: gas-phase chromatography investigating volatility of the heaviest molecules^{3,4} and aqueous chemistry experiments on complex formation by solvent extraction or ion exchange.^{2,5} The aim of these experiments is to find out whether the heaviest elements follow trends in properties found within their lighter homologues: strong relativistic effects on the outer valence electron shells are believed to result in some unexpected deviations.

The first chemical study of seaborgium in aqueous phase was its one-step elution as a neutral or anionic species in 0.1 M HNO₃/5 × 10^{−4} M HF solutions from cation exchange columns.² These experiments demonstrated Sg to behave like its lighter homologues Mo and W, forming neutral or anionic oxo- or oxofluoro complexes, and its position in group 6 was confirmed. To exclude the influence of the strong complexing action of the F[−] ions, another similar study was performed in

which the group 6 elements were eluted from the cation exchange columns in 0.1 M HNO₃ without HF.⁶ In these latter experiments, Sg was not eluted from the column in contrast to W, and this non-tungsten-like behavior of Sg was tentatively attributed to its lower tendency to hydrolyze compared to that of tungsten.

Before this work,⁶ hydrolysis of the transactinides almost has not been investigated experimentally except for one work on Rf.⁷ Theoretically, the subject has been studied by us for element 105, Db, and other group 5 elements Nb and Ta, as well as Pa, using a model based on fully relativistic density-functional calculations of hydrated and hydrolyzed species of these elements.^{8–10} Experimental work on extraction of group 5 complexes can be found in ref 11.

The electronic structures of gaseous Sg compounds and its homologues were calculated by using both the density-functional^{12–15} and effective core potentials¹⁶ methods. In this work, we extend our considerations to the solution chemistry of the group 6 cations and try to predict their hydrolyses using the same approach as in refs 8–10.

- (1) Münzenberg, G.; Hofmann, S. In *Heavy Elements and Related New Phenomena*; Greiner, W., Gupta, R. K., Eds.; World Scientific: Singapore, 1999; pp 9–42.
- (2) Schädel, M.; Brüchle, W.; Dressler, R.; Eichler, B.; Gäggeler, H. W.; Günther, R.; Gregorich, K. E.; Hoffman, D. C.; Hübener, S.; Jost, D. T.; Kratz, J. V.; Paulus, W.; Schumann, D.; Timokhin, S.; Trautmann, N.; Türler, A.; Wirth, G.; Yakushev, A. *Nature* **1997**, *388*, 55–57.
- (3) Eichler, B.; Brüchle, W.; Dressler, R.; Düllmann, Ch.; Eichler, B.; Gäggeler, H. W.; Gregorich, K. E.; Hoffman, D. C.; Hübener, S.; Jost, D. T.; Kirbach, U.; Laue, C. A.; Lavanchy, V. M.; Nitsche, H.; Patin, J.; Piguët, D.; Schädel, M.; Shaughnessy, D. A.; Strellis, D.; Taut, S.; Tobler, L.; Tsyganov, Y.; Türler, A.; Vahle, A.; Wilk, P.; Yakushev, A. *Nature* **2000**, *407*, 63.
- (4) Von Zweidorf, A.; Angert, R.; Brüchle, W.; Jäger, E.; Kratz, J. V.; Kronenberg, A.; Langrock, G.; Li, Z.; Schädel, M.; Schausten, B.; Schimpf, E.; Stiel, E.; Strub, E.; Trautmann, N.; Wirth, G. Annual Report 1999; University of Mainz: März, Germany, 2000; p 16.
- (5) Kratz, J. V. In *Heavy Elements and Related New Phenomena*; Greiner, W., Gupta, R. K.; World Scientific: Singapore, 1999; pp 129–193.

- (6) Schädel, M.; Brüchle, W.; Jäger, E.; Schausten, B.; Wirth, G.; Paulus, W.; Günter, R.; Eberhardt, K.; Kratz, J. V.; Seibert, A.; Strub, E.; Thörle, P.; Trautmann, N.; Waldek, A.; Zauner, S.; Schumann, D.; Kirbach, U.; Kubica, B.; Misiak, R.; Nagame, Y.; Gregorich, K. E. *Radichim. Acta* **1998**, *83*, 163–165.
- (7) Bilewicz, A.; Siekierski, S.; Kacher, C. D.; Gregorich, K. E.; Lee, D. M.; Stoyer, N. J.; Kadkhodayan, B.; Kreek, S. A.; Lane, M. R.; Sylwester, E. R.; Neu, M. P.; Mohar, M. F.; Hoffman, D. C. *Radichim. Acta* **1996**, *75*, 121–126.
- (8) Pershina, V. *Radichim. Acta* **1998**, *80*, 65–74.
- (9) Pershina, V. *Radichim. Acta* **1998**, *80*, 75–84.
- (10) Pershina, V.; Bastug, T. *Radichim. Acta* **1999**, *84*, 79–84.
- (11) Paulus, W.; Kratz, J. V.; Strub, E.; Zauner, S.; Brüchle, W.; Pershina, V.; Schädel, M.; Schausten, B.; Adams, J. L.; Gregorich, K. E.; Hoffman, D. C.; Lane, M. R.; Laue, C.; Lee, D. M.; McGrath, C. A.; Shaughnessy, D. K.; Strellis, D. A.; Sylwester, E. R. *Radichim. Acta* **1999**, *84*, 69–77.
- (12) Pershina, V.; Fricke, B. *Radichim. Acta* **1994**, *65*, 13–17.
- (13) Pershina, V.; Fricke, B. *J. Phys. Chem.* **1994**, *98*, 6468–6473.
- (14) Pershina, V.; Fricke, B. *J. Phys. Chem.* **1995**, *99*, 144–147.
- (15) Pershina, V.; Fricke, B. *J. Phys. Chem.* **1996**, *100*, 8748–8751.
- (16) Han, Y.-K.; Son, S.-K.; Choi, Y. J.; Lee, Y. S. *J. Phys. Chem. A* **1999**, *103*, 9109–9115.

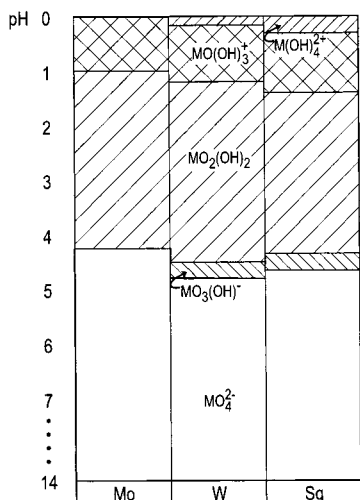
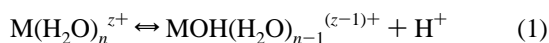


Figure 1. 1. Predominance diagram for group 6 elements in aqueous noncomplexing medium (on the basis of the diagram from ref 17).

In the next section, some aspects of the hydrolyses of Mo and W are presented. The hydrolysis model, the relativistic density-functional method, and details of the calculations are described in section III. Results are discussed in section IV. A summary is presented in section V.

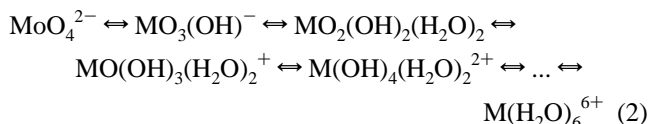
II. Hydrolysis of Group 6 Elements

Hydrolysis of cations is described as a successive loss of protons:¹⁷



Since the experiments on the heaviest elements and their homologues are conducted at a “one-atom-at-a-time” scale, our interests are limited to mononuclear species of these elements.

Group 6 elements are stable in noncomplexing solutions predominantly in the +6 oxidation state. The predominance diagram is shown in Figure 1. The “real” formulas of HMO_4^- and H_2MO_4 were proposed¹⁸ as $MO_3(OH)^-$ and $MO_2(OH)_2(H_2O)_2$, respectively, on the basis of comparisons of pK for Mo and W with those for analogous complexes of other elements. The protonation scheme then can be described as follows.



(The $M(H_2O)_6^{6+}$ species are hypothetical, but proved to be useful in the following considerations of hydrolysis.) The measured equilibrium constants^{17–24} are given in Table 1. They are indicative of a stronger hydrolysis of Mo in comparison

with that of W. Some known enthalpies and entropies of the protonation reactions are given in Table 2. For reaction 2 there, the formation of $MoO_2(OH)_2(H_2O)_2$ with coordination number (CN) 6 results in a drastic decrease in the entropy term. The protonation processes for the Sg compounds is assumed to be similar to that of Mo and W.

III. Model of Hydrolysis for Mononuclear Species

A. Hydrolysis Model. A simple hydrolysis model¹⁷ suggests that $\log K$ for reaction 1 changes linearly with the ratio of the cationic charge to the M–OH distance or the radius of the cation:

$$\log K_1 = A + \frac{B}{d_{M-OH}} z + \log 2n + \log 55.5 \quad (3)$$

The model does not, however, explain a stronger hydrolysis of Zr in comparison with that of Hf and does not explain a stronger hydrolysis of Nb in comparison with that of Ta, though the radius of Zr^{4+} (0.84 Å for CN = 8) is slightly larger than the radius of Hf^{4+} (0.83 Å) and the radius of Nb^{5+} is equal to the radius of Ta^{5+} (0.64 Å for CN = 6).²⁶ For heavier transition metal compounds with more covalent character of bonding,²⁷ eq 3 may not be reliable any more. The following proposed model^{8,9} is free of those drawbacks.

In a fashion analogous to that of Kassiakoff and Harker,²⁸ the following expression for the free energy of formation of the $M_xO_u(OH)_v(H_2O)_w^{(z-2u-v)+}$ species from the elements was adopted:

$$\frac{-\Delta G^f(u,v,w)}{2.3RT} = \sum a_i + \sum a_{ij} + \log Q - \log(u!v!w!2^w) + (2u + v + 1) \log 55.5 \quad (4)$$

The equilibrium constant is

$$\log K = \frac{-\Delta G^r}{2.3RT} \quad (5)$$

where ΔG^r is the free energy change of a hydrolysis reaction. The first term on the right-hand side of eq 4, $\sum a_i$, is the nonelectrostatic contribution from M, O, OH, and H_2O . The next term, $\sum a_{ij}$, is a sum of each pairwise electrostatic (Coulomb) interaction:

$$E^C = \sum a_{ij} = -B \sum_{ij} Q_i Q_j / d_{ij} \quad (6)$$

where d_{ij} is the distance between moieties i and j , Q_i and Q_j are their effective charges, $B = 2.3RTe^2/\epsilon$ is an independent constant, and ϵ is the effective dielectric constant. Q is the partition function representing the contribution of structural isomers if there are any. The last two terms in eq 4 are statistical; one is a correction for the indistinguishable configurations of the species, and the other is a conversion to the molar scale of concentration for the entropy.

$\sum a_{ij}$ and $\sum a_i$ for each compound are obtained from electronic density distribution data calculated using the fully relativistic density-functional method described below. The differences in those values for the left and the right parts of the equilibrium reactions plus the differences in the other terms of eq 4 will

(17) Baes, C. F., Jr.; Mesmer, R. E. *The Hydrolysis of Cations*; John Wiley: New York, 1976.

(18) Tytko, K. H. *Polyhedron* **1986**, *5*, 497–503.

(19) Rohwer, E. F. C. H.; Cruywagen, J. J. *J. S. Afr. Chem. Inst.* **1964**, *XVII*, 145–148.

(20) Rohwer, E. F. C. H.; Cruywagen, J. J. *J. S. Afr. Chem. Inst.* **1966**, *XIX*, 11–23.

(21) Cruywagen, J. J.; Heyns, J. B. B.; Rohwer, E. F. C. H. *J. Inorg. Nucl. Chem.* **1976**, *38*, 2033–2034.

(22) Tytko, K. H.; Glemser, O. *Adv. Inorg. Chem. Radiochem.* **1976**, *19*, 239–315.

(23) Sasaki, J.; Sillen, L. G. *Acta Chem. Scand.* **1964**, *18*, 1014–1019.

(24) Schwarzenbach, G. *Pure Appl. Chem.* **1962**, *5*, 377–380.

(25) Arnek, R.; Szilard, I. *Acta Chem. Scand.* **1968**, *22*, 1334–1338.

(26) Shannon, R. D. *Acta Crystallogr., Sect. A* **1976**, *32*, 751–767.

(27) Pershina, V. *Chem. Rev.* **1996**, *96*, 1977–2010.

(28) Kassiakoff, A.; Harker, D. *J. Am. Chem. Soc.* **1938**, *60*, 2047–2055.

Table 1. Consecutive Protonation Equilibria and Constants for the Group 6 Complexes (for Mo and W from Ref 22)

step	equilibrium	log K_n (Mo)	log K_n (W)	log K_n (Sg) ^h
I	$\text{MO}_4^{2-} + \text{H}^+ \rightleftharpoons \text{MO}_3(\text{OH})^-$	3.7 ^a	3.8 ^b	3.74
II	$\text{MO}_3(\text{OH})^- + \text{H}^+ + 2\text{H}_2\text{O} \rightleftharpoons \text{MO}_2(\text{OH})_2(\text{H}_2\text{O})_2$	3.8 ^c	4.3 ^d	3.9–4.3
I + II	$\text{MO}_4^{2-} + 2\text{H}^+ + 2\text{H}_2\text{O} \rightleftharpoons \text{MO}_2(\text{OH})_2(\text{H}_2\text{O})_2$	7.50 ^e	~8.1 ^f	7.8–8.0
III	$\text{MO}_2(\text{OH})_2(\text{H}_2\text{O})_2 + \text{H}^+ \rightleftharpoons \text{MO}(\text{OH})_3(\text{H}_2\text{O})_2^+$	0.93 ^g	0.98 ^h	1.02
IV	$\text{MO}(\text{OH})_3(\text{H}_2\text{O})_2^+ + \text{H}^+ \rightleftharpoons \text{M}(\text{OH})_4(\text{H}_2\text{O})_2^{2+}$			
VI	$\text{M}(\text{OH})_4(\text{H}_2\text{O})_2^{2+} + 4\text{H}^+ \rightleftharpoons \dots \rightleftharpoons \text{M}(\text{H}_2\text{O})_6^{6+}$			

^a The other values are 3.89²³ in NaClO_4 and 4.21 in HCl .²⁰ ^b The other value is 3.5 in 0.1 M NaClO_4 .²⁴ ^c The other value is 4.0 in HCl .²⁰ ^d The other value is 4.05 in NaClO_4 .²⁴ ^e In 3 M NaClO_4 ;¹⁹ 4.11 in HCl .²⁰ ^f In 0.1 M NaClO_4 .²⁰ ^g In 0.5 M HCl (see also references in ref 21); 1.06 in 3 M NaClO_4 ;²¹ 0.934 in HCl .²⁰ ^h This work.

Table 2. Enthalpy and Entropy of Mo(VI) Equilibria in 3 M NaClO_4

	reaction	ΔH (kJ/mol)	ΔS (J/(mol K))	ref
1	$\text{MoO}_4^{2-} + \text{H}^+ \rightleftharpoons \text{MoO}_3(\text{OH})^-$	58.6 ± 29	271 ± 96	25
2	$\text{MoO}_3(\text{OH})^- + \text{H}^+ + 2\text{H}_2\text{O} \rightleftharpoons \text{MoO}_2(\text{OH})_2(\text{H}_2\text{O})_2$	-68.2	-156.1	this
3	$\text{MoO}_2(\text{OH})_2(\text{H}_2\text{O})_2 + \text{H}^+ \rightleftharpoons \text{MoO}(\text{OH})_3(\text{H}_2\text{O})_2^+$	5.98 ± 1.21	40.0 ± 8	21

define log K . The source of uncertainty in calculating E^C (eq 6) is ϵ . Therefore, for clarity, the energy of the Coulomb interaction in a vacuum will be calculated and given in the tables. The value of ϵ , or B , will be defined by using a fitting procedure described in section IV.B.

The last contribution to ΔG^r would be a change in the hydration energy ΔG_{hydr} beyond the first coordination sphere. Since the reactions in eq 2 have the same metal atom in the left and right parts, the ΔG_{hydr} should be very similar for all the elements and will not change the relative values of ΔG^r in the row Mo–W–Sg.

B. Fully Relativistic Density-Functional Method. The method at our disposal is the fully relativistic density functional with the general gradient approximation (GGA) for the exchange–correlation potential.²⁹ It has been extensively used by us for calculations of the electronic structure and bonding of numerous transactinide compounds,²⁷ so that its description can be found elsewhere.^{29,30}

The method uses four-component basis functions that are transformed into molecular symmetry orbitals using double point groups. Molecular integrals between these functions are calculated in a numerical, three-dimensional grid. The version of the method used here includes minimization of the error in the total energy³⁰ and the integration scheme of Boerrigter et al.,³¹ which altogether gives quite accurate results for total energies. Nevertheless, the geometry optimization of complicated and charged complexes in solutions did not seem to be feasible and/or efficient. Therefore, the geometry and bond lengths have been taken as described in the next subsection.

The complexes were considered without embedding, since the latter would have introduced more uncertainty in the results because of lack of knowledge of the nature and geometry of the surrounding. When hydrolysis constants are calculated, the effect of the surrounding will, however, be taken into account by a fitting procedure described in section IV.B.

The Mulliken population analysis³² was applied for the electronic density distribution. Effective charge, Q_M , and overlap population, OP, which is a direct counterpart of the covalent part of the binding energy, were then used to calculate $E^C =$

Table 3. Average M–O (M = Mo, W, and Sg) Bond Distances as a Function of CN and the Number of Terminal Oxygen Atoms, O_t (in Å)

bond	$O_t = 1$	$O_t = 2$	$O_t = 3$	$O_t = 4$
	CN = 6 $\text{MO}(\text{OH})_3(\text{H}_2\text{O})_2^+$	CN = 6 $\text{MO}_2(\text{OH})_2(\text{H}_2\text{O})_2$	CN = 4 $\text{MO}_3(\text{OH})^-$	CN = 4 MO_4^{2-}
Mo– O_t ^a	1.67	1.70	1.74	1.77
Mo–OH	1.96	1.96	1.76	
Mo– H_2O ^a	2.25	2.25		
W– O_t	1.68	1.71	1.75	1.78
W–OH	1.97	1.97	1.77	
W– H_2O	2.26	2.26		
Sg– O_t	1.72	1.75	1.80	1.83
Sg–OH	2.02	2.02	1.82	
Sg– H_2O	3.31	2.31		

^a Average distances from the data of ref 33. For the M– H_2O distances, the compounds mostly related to those indicated in the table have been selected.

$\sum a_{ij}$ and OP = $k\sum a_i$ in eq 4, respectively. For a chemical reaction,

$$\Delta E^{\text{OP}} = \Delta \sum a_{ij} = k \Delta \text{OP} \quad (7)$$

where k is a coefficient that could also be defined by a fitting procedure as is shown below.

The correct application of the Mulliken analysis requires the use of minimal consistent basis sets for all the members of the series. Therefore, the minimal basis sets including valence $ns_{1/2}$, $np_{1/2}$, $np_{3/2}$, $(n-1)d_{3/2}$, and $(n-1)d_{5/2}$ orbitals were used for all the elements. The calculations were performed within the frozen core approximation. The number of integration points was 10^4 .

C. Geometrical Configurations and Bond Distances. The M–O bond lengths used in the calculations were deduced from a careful analysis of the measured bond lengths^{33–36} for Mo and W species. They are summarized in Table 3. The data show a clear dependence of M–O distances on coordination number (CN) and the number of terminal oxygen atoms. In the case of missing data for W, the bond lengths were assumed to be 0.01 Å longer than those of Mo.²⁶ An increase in the bond lengths of the Sg compounds in relation to those of the W homologues was taken as 0.05 Å on average, as was calculated for some gaseous Sg and W molecules.¹⁶ A sum of ionic radii was taken

(29) Varga, S.; Engel, E.; Sepp, W.-D.; Fricke, B. *Phys. Rev. A* **1999**, *59*, 4288–4294.

(30) Bastug, T.; Sepp, W.-D.; Kolb, D.; Fricke, B.; Baerends, E. J.; Te Velde, G. *J. Phys. B: At. Mol. Opt. Phys.* **1995**, *28*, 2325–2332.

(31) Boerrigter, P. M.; te Velde, G.; Baerends, E. J. *Int. J. Quantum Chem.* **1988**, *33*, 87–93.

(32) Mulliken, R. S. *J. Chem. Phys.* **1955**, *23*, 1833–1840.

(33) Schröder, F. A. *Acta Crystallogr.* **1975**, *B31*, 2294–2309.

(34) Griffith, W. P. *Coord. Chem. Rev.* **1970**, *5*, 459–517.

(35) Stiefel, E. I. *Progress in Inorganic Chemistry*; Lippard, S. J., Ed.; J. Wiley and Sons: New York, 1977; Vol. 22, pp 1–211.

(36) Cotton, F. A.; Wing, R. M. *Inorg. Chem.* **1965**, *4*, 867–887.

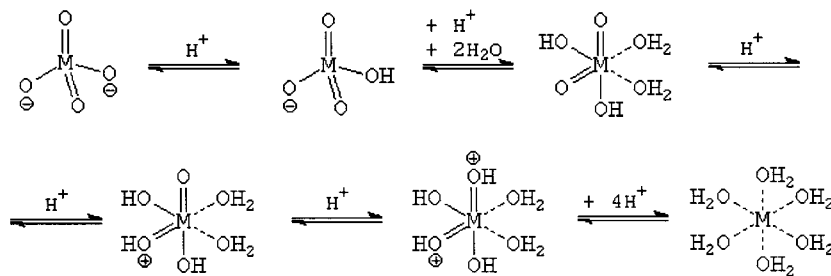


Figure 2. Geometrical configurations of the group 6 complexes in the protonation reactions.

Table 4. Energies of HOMO, LUMO, and ΔE for $\text{MO}_2(\text{OH})_2(\text{H}_2\text{O})_2$, Where M = Mo, W, and Sg

energy, eV	Mo	W	Sg
$E(\text{HOMO})$	-4.25	-3.95	-4.12
$E(\text{LUMO})$	-1.69	-0.97	-1.02
ΔE	2.57	2.99	3.10

for M–OH and M–H₂O distances.²⁶ We have also checked the influence of the bond length variation on bonding. All the variations within a fraction of an angstrom did not, however, influence relative values of ΔG^{\ddagger} in the row Mo–W–Sg. The geometrical configurations are shown in Figure 2 (O_h symmetry group for CN = 6 and T_d for CN = 4). For $\text{M}(\text{H}_2\text{O})_6^{6+}$, the T_h symmetry group is taken with the positions of the atoms shown in Figure 2 of ref 8.

IV. Results of the Calculations and Discussion

A. Energy Levels and Electronic Density Distribution. The present calculations for the aqueous species of the group 6 elements have shown trends in the electronic structure and bonding to be very similar to those obtained for the group 6 gas-phase compounds.^{12–16} In Table 4, the energies of the highest occupied MO (HOMO), the lowest unoccupied MO (LUMO), and the energy gap, ΔE , between them are given for $\text{MO}_2(\text{OH})_2(\text{H}_2\text{O})_2$, as an example. The electronic density distribution data, Q_M , OP, and E^C obtained as a result of the calculations are given in Table 5. One can see an increase in the covalence and a decrease in the ionicity of the metal–ligand bond from Mo to Sg. This increase is caused by the relativistic contraction and stabilization of the 7s and 7p_{1/2} valence orbitals, leading to their enhanced participation in the chemical bonding.^{12–15} The increasing values of Q_M in the protonation process for each element (Table 5) reflect a trend of an increase in the ionicity of the compounds with increasing number of the OH[−] groups.

ΔE^C and ΔOP for the protonation process calculated on the basis of the values of Table 5 are given in Table 6. Positive values of ΔOP mean an increase in the covalent interaction energy, so a negative energy change ΔE^{OP} occurs. Comparing ΔE^C of Table 6 for the first two protonation steps (predominantly covalent complexes), one can see an extremum on W; the largest negative values of ΔE^C mean its strongest preference for protonation, or the weakest preference for hydrolysis, which is in agreement with the experimental results (see Table 1). Thus, for the first two protonation steps involving more covalent compounds the trend is reversed: $\text{W} > \text{Sg} > \text{Mo}$. It is interesting to note here that this reversed trend is similar to the one for the formation of chloro, bromo, and fluoro complexes of group 5 elements, which was predicted theoretically^{9,10} and confirmed experimentally.¹¹ For further protonation processes with the formation of the positively charged complexes, ΔE^C becomes smoothly more negative from Mo to W and to Sg so that the trend is $\text{Sg} > \text{W} > \text{Mo}$.

B. Predictions of Hydrolysis/Protonation Constants for Sg.

It is also possible to give absolute values of the protonation constants for Sg using $\log K$ for Mo and W from Table 1. Thus, with use of eqs 4–6 and 7, $\log K$ for the I, II, I + II, and III protonation steps are

$$\log K_1 = k \Delta\text{OP} + B' \Delta E^C - 1.142 \quad (8)$$

$$\log K_2 = k \Delta\text{OP} + B' \Delta E^C + B'' 2D_{\text{H}_2\text{O}} - 2.464 \quad (9)$$

$$\log K_1 + \log K_2 = k \Delta\text{OP} + B' \Delta E^C + B'' 2D_{\text{H}_2\text{O}} - 3.613 \quad (10)$$

$$\log K_3 = k \Delta\text{OP} + B' \Delta E^C - 0.176 \quad (11)$$

where B' and k correct not only for the unknown dielectric constant in solution but also for the fact that the E^C values were calculated for the species in a vacuum, as was mentioned earlier.

Thus, for the first protonation step, the two following equations with two unknown parameters should be solved using the data of Table 6:

$$\log K_1(\text{Mo}) = 0.16k + 12.98B' - 1.142 = 3.7 \quad (12)$$

$$\log K_1(\text{W}) = 0.12k + 13.13B' - 1.142 = 3.8 \quad (13)$$

Their solution gives $B' = 0.38$ and $k = -1.0$. Using then ΔOP and ΔE^C for Sg from Table 6, we obtain

$$\log K_1(\text{Sg}) = 0.11k + 12.95B' - 1.142 = 3.74 \quad (14)$$

In a similar way, the protonation constant was defined for the second protonation step (see Table 1 and eq 9), where $B' = B'' = 1.64$, $k = 4.22$, and $D(\text{H}_2\text{O}, \text{aq}) = 10.70$ eV. Another way to obtain $\log K_1 + \log K_2$ would be to solve eq 10 for Mo and W. This would give $k = 2.19$ and $B' = 0.58$. By use of these values, $\log K_1 + \log K_2 = 7.6$ for Sg.

We have also calculated the first and second protonation constants for Sg by varying the metal–water bond lengths, which might be longer than those given in Table 3. An increase in the bond lengths of up to 2.37 Å for Mo, 2.38 Å for W, and 3.43 Å for Sg results in a decrease in the protonation constant for Sg down to $\log K_2 = 3.94$. This would give $\log K_1 + \log K_2 = 7.79$ for this element. The calculated values of $\log K$ for Sg are summarized in Table 1. The obtained $\log K$ and $\log K_1 + \log K_2$ for Sg are indicative of the same trend in hydrolysis as the ΔE^C data show: $\text{Mo} > \text{Sg} > \text{W}$.

Thus, it is worth stressing again that even though the covalent effects become predominant within the transition element groups with increasing atomic number, the changes in the electrostatic metal–ligand interaction do define the hydrolysis process.^{8–10}

Table 5. Q_M , E^C (in eV), and OP for Group 6 Complexes^a

	$MO_4^{2- b}$	$MO_3(OH)^-$	$MO_2(OH)_2(H_2O)_2$	$MO(OH)_3(H_2O)_2^+$	$M(OH)_4(H_2O)_2^{2+}$	$M(H_2O)_6^{6+}$
$Q(Mo)$	0.36	0.83	1.23	1.48	1.66	2.08
$Q(W)$	0.43	0.88	1.29	1.55	1.73	2.21
$Q(Sg)$	0.32	0.80	1.19	1.47	1.67	2.18
$E^C(Mo)$	3.51	-9.47	-30.90	-36.74	-37.17	4.80
$E^C(W)$	2.62	-10.51	-32.60	-38.95	-39.71	-0.80
$E^C(Sg)$	3.86	-9.09	-30.70	-37.35	-38.58	-1.45
OP(Mo)	2.59	2.76	4.23	4.86	5.62	6.42
OP(W)	3.09	3.21	4.69	5.33	6.06	6.87
OP(Sg)	3.15	3.26	4.80	5.46	6.22	7.08

^a One should not be confused by the large values of E^C for some compounds. This is the Coulomb part of the atomization energy. Thus, for example, the atomization energy of $MoO_2(OH)_2(H_2O)_2 \rightarrow M + 6O + 6H$ calculated via the Born-Haber cycle for the formation of " H_2MoO_4 "(aq)³⁷ is 45.88 eV, so $E^C = 30.9$ eV is indicative of a 60% ionic bonding. ^b Positive E^C values are due to the absence of embedding.

Table 6. ΔE^C and ΔOP for the Stepwise Protonation of MO_4^{2-} (M = Mo, W, and Sg)

reaction	ΔE^C , eV			ΔOP		
	Mo	W	Sg	Mo	W	Sg
$MO_4^{2-} + H^+ \leftrightarrow MO_3(OH)^-$	-12.98	-13.13	-12.95	0.16	0.12	0.11
$MO_3(OH)^- + H^+ + 2H_2O \leftrightarrow MO_2(OH)_2(H_2O)_2$	-21.43	-22.08	-21.61	1.47	1.49	1.54
$MO_2(OH)_2(H_2O)_2 + H^+ \leftrightarrow MO(OH)_3(H_2O)_2^+$	-5.84	-6.35	-6.65	0.63	0.64	0.66
$MO(OH)_3(H_2O)_2^+ + H^+ \leftrightarrow M(OH)_4(H_2O)_2^{2+}$	-0.43	-0.76	-1.23	0.76	0.73	0.77
$M(OH)_4(H_2O)_2^{2+} + 4H^+ \leftrightarrow \dots \leftrightarrow M(H_2O)_6^{6+}$	41.97	38.71	37.11	0.80	0.81	0.85

The following relations confirm this.

$$Mo: \log K_1/\Delta E^C_1 = 3.7/12.98 = 0.29 \quad (15)$$

$$W: \log K_1/\Delta E^C_1 = 3.8/13.13 = 0.29 \quad (16)$$

$$Mo: [\log K_1 + \log K_2]/[\Delta E^C_1 + \Delta E^C_2] = 7.50/34.01 = 0.22 \quad (17)$$

$$W: [\log K_1 + \log K_2]/[\Delta E^C_1 + \Delta E^C_2] = 8.1/35.21 = 0.23 \quad (18)$$

Thus, by use of the fact that $\log K_n/\Delta E^C_n = \text{const}$, and knowing ΔE^C for the Sg reactions, the related constants for Sg can be defined as $\log K_1 = 3.73$ and $\log K_1 + \log K_2 = 7.5-7.9$, which are very close to those given in Table 1.

By using this well-established proportionality, we can define $\log K_3$ for W and Sg knowing only the ratio $\log K_3/\Delta E^C_3 = 0.93/5.84 = 0.16$ for Mo and ΔE^C_3 for W and Sg (Table 6). This would give $\log K_3(W) = 0.98$ and $\log K_3(Sg) = 1.02$ (Table 1). If we use another value of $\log K_3(Mo) = 1.06$ for 3 M NaClO₄, we obtain $\log K_3(W) = 1.15$ and $\log K_3(Sg) = 1.21$. Thus, for step III the trend in the protonation is the following: Sg > W > Mo. For the next protonation steps, the calculations show Sg to be even more easily protonated than Mo and W, so its hydrolysis is much weaker. A summary diagram for all group 6 elements is shown in Figure 1.

The trend in the hydrolysis of the group 6 cations at pH = 1 obtained as a result of the present calculations is in agreement with the recent experimental results on elution of W and Sg from cation exchange columns in 0.1 M HNO₃.⁶ Obviously, Sg, being in the positively charged form, was not eluted from the column in contrast to W, being in the form of the neutral complex.

(37) Wagman, D. D.; Evans, W. H.; Parker, V. B.; Schumm, R. H.; Halow, I.; Bailey, S. M.; Churney, K. L.; Nuttall, R. L. *J. Phys. Chem. Ref. Data* **1982**, *11* (Suppl. 2).

V. Conclusions

Relativistic density-functional calculations of the electronic structure of hydrated and hydrolyzed species of Mo, W, and Sg in aqueous solutions and derived protonation constants have shown hydrolysis of the neutral species with the formation of the negative oxo complexes to have the reversed trend in the chemical group: Mo > Sg > W. An analogous trend was observed for the complex formation of group 5 elements in HCl, HBr, and HF solutions: Nb > Db > Ta.⁹⁻¹¹

For the positively charged complexes in equilibrium with the neutral complexes, the trend of a decrease in hydrolysis from Mo to W continues further for Sg: Mo > W > Sg. This result is in agreement with the experimental data on hydrolysis of Mo and W¹⁷ and, recently, on Sg.⁶

A decisive factor in the protonation/hydrolysis processes proved to be the predominant changes in the electrostatic metal-ligand interaction energy of the equilibrium reactions. Thus, in going in the periodic table from the 4d and 5d elements to the 6d elements, electrostatics will still define the nature of the metal-ligand interactions and, eventually, the hydrolysis process. Nevertheless, the electrostatic, as well as nonelectrostatic interactions, must be determined on the basis of results of relativistic molecular calculations. Using formal effective charges as those used in the simple hydrolysis model can lead to erroneous results.

The present calculations have also demonstrated that linear extrapolations of properties are no more reliable in the area of the very heavy elements.

Acknowledgment. V.P. gratefully acknowledges the financial support of the Deutsche Forschungsgemeinschaft (DFG) under Contract KR1458/5-1. The calculations were performed on an IBM-AIX cluster of the Gesellschaft für Schwerionenforschung, Darmstadt. The version of the density-functional program used here was developed by the group of Prof. B. Fricke, University of Kassel, whom the authors thank for the support of the research.

IC0003731